CHARTS FOR PRELIMINARY SELECTION OF NU GIRDER SECTIONS BASED ON KANSAS DEPARTMENT OF TRANSPORTATION LRFD DESIGN GUIDELINES FOR PRESTRESSED CONCRETE BEAMS

By:

Kelly Carlton

Rémy Lequesne

Structural Engineering and Engineering Materials

SL Report 16-2

THE UNIVERSITY OF KANSAS CENTER FOR RESEARCH, INC.

LAWRENCE, KANSAS

May 2016

ABSTRACT

The Kansas Department of Transportation, which currently uses a series of standard prestressed concrete beam sections referred to as K-girders for prestressed beam bridge projects, is considering a switch to use of NU I-girder sections. The NU I-Girder sections are attractive for their efficiency, but Kansas engineers are not accustomed to their use. The aim of this analytical study was to develop an Excel-based tool that can be used to produce charts that engineers can use for preliminary selection of NU I-girder section sizes and strand numbers. The calculations described herein are in compliance with KDOT Bridge Design Specifications.

ACKNOWLEDGEMENTS

This report is based on calculations performed by Kelly Carlton to fulfill the project requirement of the Master of Science in Civil Engineering degree at the University of Kansas as well as the request of the Kansas Department of Transportation. Project guidance and review of calculations were provided by Mr. Calvin Reed, P.E., former State Bridge Design Engineer and Assistant Bureau Chief of the Kansas Department of Transportation Bureau of Structures and Geotechnical Services, and Rémy Lequesne, Ph.D., P.E., Assistant Professor of Civil, Environmental and Architectural Engineering at the University of Kansas.

1. INTRODUCTION

The Kansas Department of Transportation (KDOT) currently uses a series of standard prestressed concrete beam sections, referred to as K-girders, for prestressed beam bridge projects throughout the State of Kansas. The K-girders were developed from the American Association of State Highway and Transportation (AASHTO) standard sections. Figures 1 - 4 show the geometry and possible strand configurations for several of the K-girders.

In the 1990s, a cooperative effort between the Center for Infrastructure Research at the University of Nebraska and the Nebraska Department of Roads (NDOR) led to the development of an alternative set of standard beam sections, referred to as NU girders. Figure 5 and Table 2 show the geometry and strand locations for the NU girder prestressed beam sections.

The geometry of NU girder sections, along with the use of high-strength concrete, allow for the construction of longer spans than possible with other standard prestressed beam sections (e.g. AASHTO, PCI, or K-girder sections). The wide top flange creates shorter deck spans between beams and provides a wider platform for workers during construction. The wide and thick bottom flange allows for increased strand capacity for resisting positive moment demands and a larger compression flange for resisting negative moment demands. The wide bottom flange also provides increased stability during shipping and handling. Furthermore, the curved fillets reduce stress concentrations. Other features of the design, including standard bottom and top flange dimensions, result in reductions in fabrication time and formwork cost.

The length of a bridge is controlled by horizontal and vertical clearances. The large span-to-depth ratios possible when NU girder sections are used in design and their relative cost-efficiency make them a good alternative to steel girder sections traditionally used for longer spans. The ability to span longer distances with the NU girders also aids in minimizing the number of substructure components for a bridge and creates a more efficient system. It may also help avoid locating a pier in the middle of a stream. Table 2.1.1-1 in the KDOT Bridge Design Manual suggests “efficient” length of span ranges based on design experience for various bridge types. Table 1 displays this information for the most common bridge types used by KDOT engineers for in-house design.

Table 1 – KDOT "Efficient" Length of Span Range

Superstructure Type	Length of Span (ft)
Structural Steel Plate Girder (Composite)	80 - 240
Steel Rolled Beam (Composite)	40 - 120
K-2 Prestressed Concrete Girder (Composite)	40 - 60
K-3 Prestressed Concrete Girder (Composite)	50 - 70
K-4 Prestressed Concrete Girder (Composite)	60 - 100
K-6 Prestressed Concrete Girder (Composite)	80 - 120
Reinforced Concrete Haunched Slab	30 - 65

Charts are available (Hanna et al. 2010) that allow for preliminary selection of NU girder sections conforming to Nebraska Department of Roads (NDOR) design specifications. Because the Kansas Department of Transportation (KDOT) is moving towards adoption of NU girder sections for in-house projects, in addition to the consultant projects where they are already being used, there is a need for similar design aids to allow for selection of NU girders conforming to KDOT design specifications. KDOT engineers wanted to have a tool for developing their own charts similar to those published in the NDOR report. The aim of this report is to describe the process of developing such charts and to provide a sample of the design aids that can be produced using the methods described.

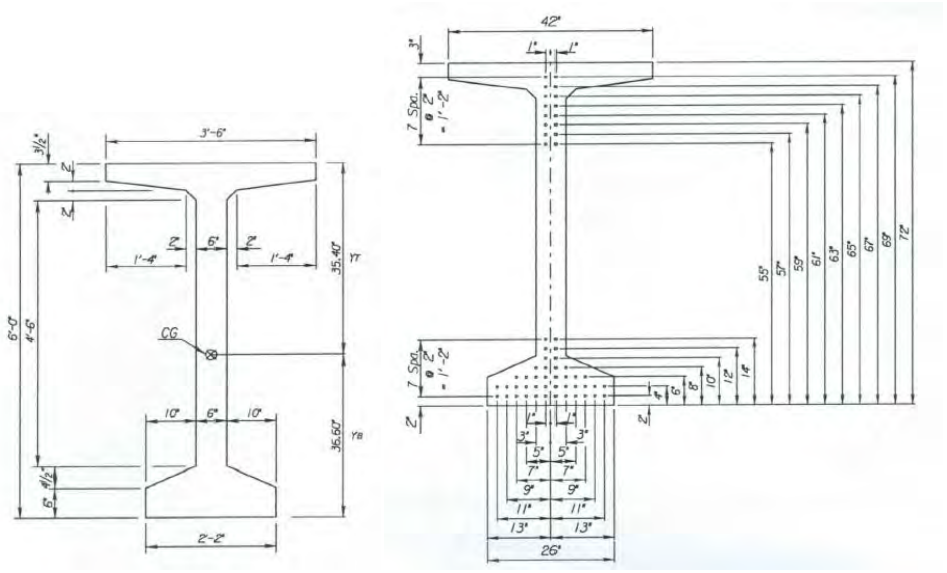

Figure 1 - K-6 girder geometry and strand layout (KDOT 2016)

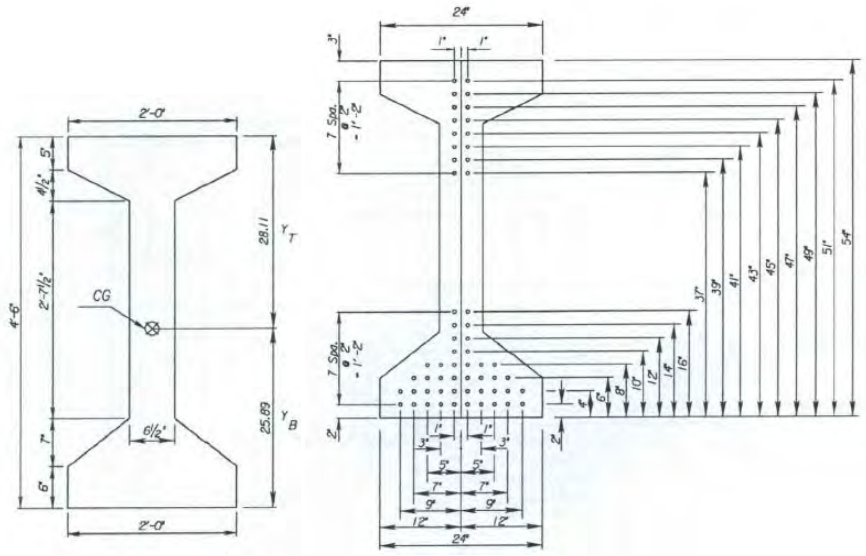

Figure 2 – K-4 girder geometry and strand layout (KDOT 2016)

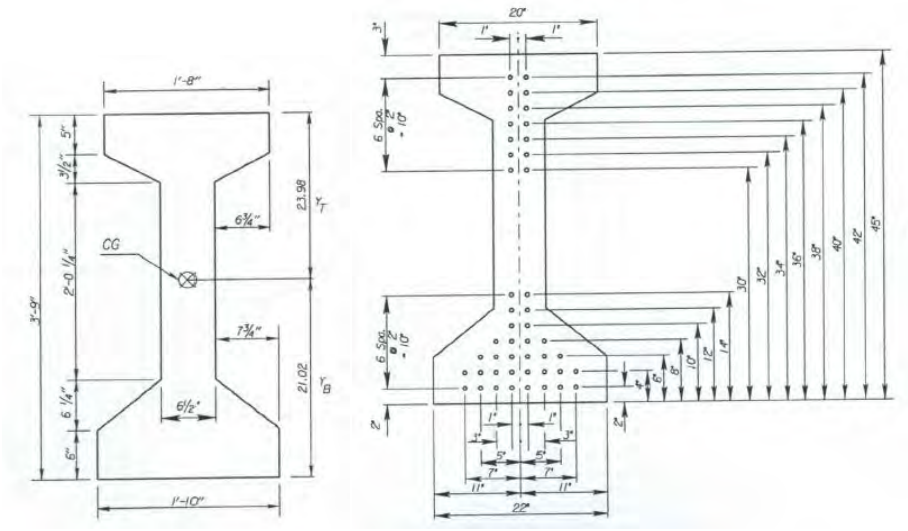

Figure 3 - K-3 girder geometry and strand layout (KDOT 2016)

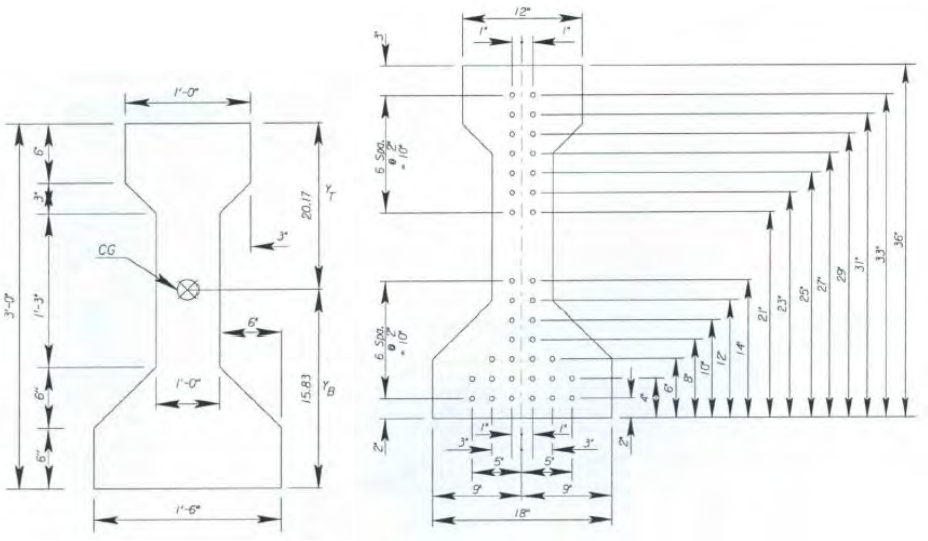

Figure 4 - K-2 girder geometry and strand layout (KDOT 2016)

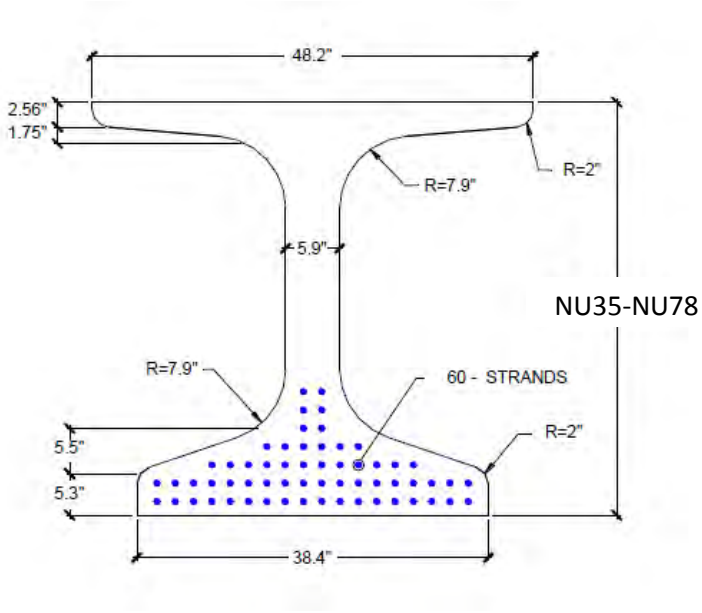

Figure 5 – NU girder section

Table 2 – NU Girder Section Dimensions and Properties

Section	Height (in)	Web Width (in)	Top Flange Width (in)	Bottom Flange Width (in)	Area (in^2)	Y_b (in)	I (in^4)	Weight (kips/ft)
NU35	35.4	5.9	48.2	38.4	648.1	16.1	110262	0.680
NU43	43.3	5.9	48.2	38.4	694.6	19.6	182279	0.724
NU53	53.1	5.9	48.2	38.4	752.7	24	302334	0.785
NU63	63	5.9	48.2	38.4	810.8	28.4	458482	0.840
NU70	70.9	5.9	48.2	38.4	857.3	32	611328	0.894
NU78	78.7	5.9	48.2	38.4	903.8	35.7	790592	0.942

Note: The option to add one, two, or three inches of concrete thickness to the top of the beam top flange was included in the calculations for this project.

2. Outline of Analytical Study

2.1. Aim and Scope

The aim of this analytical study was to develop an Excel-based tool that can be used to develop charts that are useful to engineers doing preliminary selection of NU girder section sizes and strand numbers for bridges designed in accordance with KDOT specifications. The tool can be used to develop two types of charts. The first type shows the span lengths attainable for a specific NU section, girder spacing, and concrete compressive strength. The second chart type shows the number of strands required to attain a given span length for a given NU section, girder spacing, and concrete compressive strength. As stated previously, such charts are available (Hanna et al. 2010) that were developed in accordance with Nebraska Department of Roads (NDOR) design specifications. Examples of each type of figure, taken from the Hanna et al. report, are reproduced as Figures 6 and 7 below.

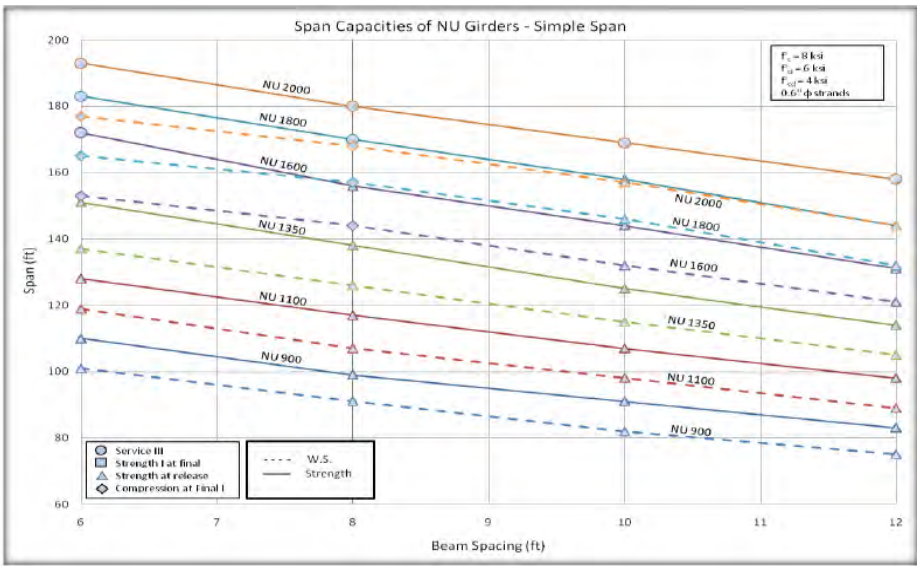

Figure 6 – Maximum possible span for given NU girder section and girder spacing (Hanna et al. 2010)

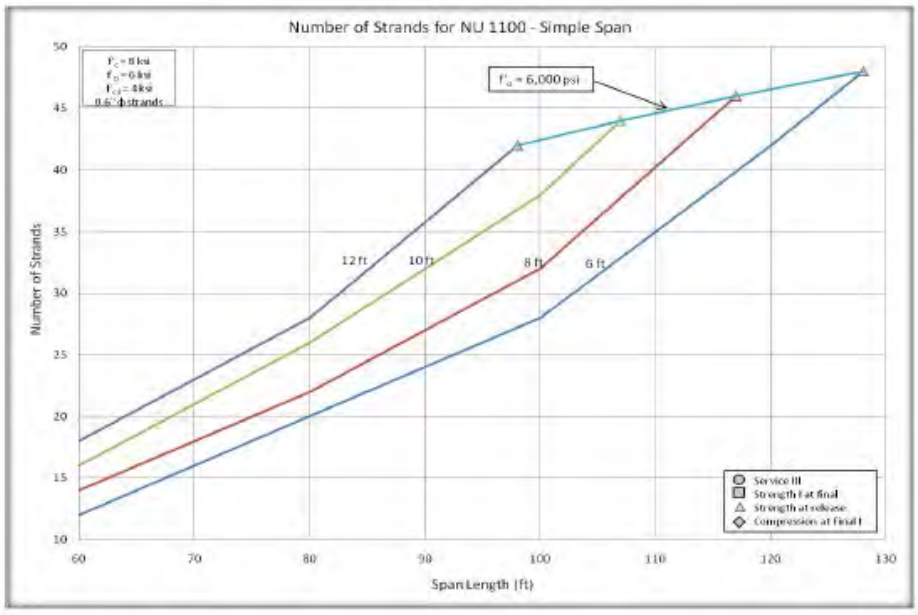

Figure 7 – Minimum number of strands for a given NU girder section and span (Hanna et al. 2010)

The analyses reported herein were based on the following design specifications and guidelines:

- AASHTO LRFD Bridge Design Specifications, Seventh Edition, 2014 with 2015 Interims
- Kansas Department of Transportation Bridge LRFD Design Manual.

The following three limit states were considered in the reported analyses. Each will be described later in the report in greater detail.

- Strength I
- Service I
- Service III

The scope of the analysis was limited by the following assumptions. Although not every design condition is included within the following ranges, the scope of variables were selected to include conditions most likely to be observed in practice.

Evaluation ranges and design criteria:

- Simple Span
- Interior Girders
- NU girder sections: NU35, NU43, NU53, NU63, NU70, and NU78
- Beam Spacing: 6, 8, 10 and 12 ft

- Final compressive strength of concrete used to construct NU girders: 6, 7, 8, 9 and 10 ksi
- Compressive strength of NU girder concrete at release, $f'_{ci} = 0.75f'_c$
- Compressive strength of concrete used to construct bridge decks: 4 ksi
- Deck thickness of 8.5 in. with a 0.5 in. sacrificial wearing surface
- Fillet thickness of 1.5 in.
- Grade 270 (f_{pu} = 270 ksi) low-relaxation prestressing strands with an assumed modulus, E_s, of 28,500 ksi and yield strength, f_{py}, of 243 ksi
- Jacking stress = $0.75f_{pu}$
- Prestressing strand diameter of 0.6 in.
- Strand number limited to 60
- Fully bonded straight strands, debonded strands and harped strands
- Dead Loads include beam weight, deck and fillet weight, bridge rail weight, and future wearing surface
- Live Loads include HL-93 loading

2.2. Design Basis and Limit States

The main goal of engineering design is that the capacity of a structure to resist loads, or the resistance, is equal to or greater than the demand on the structure from loading. This can be stated as:

$$Resistance \geq Loads \qquad \text{Eq. 1}$$

The AASHTO LRFD Bridge Design Specifications apply factors to both the resistance and load side of the equation to increase the safety of the design. These factors account for uncertainty and variability in the loading on a bridge structure as well as uncertainty in the resistance of the structure considering variability in materials and construction quality, and uncertainty in calculation methods. The following is the design equation used by LRFD that must be satisfied for all limit states (Barker and Puckett 2007):

$$\Sigma\eta_i\gamma_i Q_i \leq \varphi R_n \qquad \text{Eq. 2}$$

Where:

Q_i = force effect

R_n = calculated nominal resistance

γ_i = statistically based load factor

φ = statistically based resistance factor

η_i = load modification factor

Following AASHTO LRFD Eq. 1.3.2.1-2, when a maximum value of γ_i is appropriate the load modification factor, η_i, is determined using Eq. 3.

$$\eta_i = \eta_D \eta_R \eta_I \geq 0.95 \quad \text{Eq. 3}$$

Where:

η_D = ductility factor

η_R = redundancy factor

η_I = operational importance factor

Assuming typical bridge details, η_i was taken as 1.0 for all limit states on this project. AASHTO LRFD Sections 1.3.3, 1.3.4, and 1.3.5 give values for the ductility, redundancy and operational importance factors.

The AASHTO LRFD specifications give limit states for design comprised of factored load combinations. A limit state is defined as "a condition beyond which a bridge system or bridge component ceases to fulfill the function for which it is designed." The prestressed beams for the project were checked for the strength limit state (Strength I) and also for service limit states (Service I and III) meant for limiting stresses in the beams. Each of these limit states is defined for specific load combinations (Tables 3.1 and 3.2 in the AASHTO LRFD Specifications) and design checks. The following briefly describes the limit states and associated factored load combinations used to evaluate NU girders in this project.

Strength I Limit State

The Strength I limit state relates to "normal vehicular use of the bridge without wind" (AASHTO LRFD Article 3.4.1). This limit state was used to evaluate the flexural strength of the prestressed beams. The pertinent load combination given in AASHTO LRFD Table 3.1 is given in Eq. 4.

$$\gamma_p DC + \gamma_p DW + 1.75(LL + IM) \quad \text{Eq. 4}$$

Where:

γ_p = load factor (Table 3)

DC = Dead load from structural components and nonstructural attachments

DW = Dead load from wearing surfaces and utilities

LL = Vehicular live load

IM = Vehicular dynamic load allowance

Table 3 - Load factors, γ_p (AASHTO LRFD Table 3.2)

Type of Load	Maximum Load Factor
DC	1.25
DW	1.50

Substitution of factors given in Table 3 into Eq. 4 results in Eq. 5.

$$1.25DC + 1.50DW + 1.75\ (LL + IM) \qquad \text{Eq. 5}$$

AASHTO LRFD Article 5.5.4.2.1 defines the strength resistance factor, φ, for the strength limit state for reinforced concrete sections. Figure 8 shows the variation in the φ-factor for prestressed concrete sections as a function of the tensile strain calculated in the reinforcement.

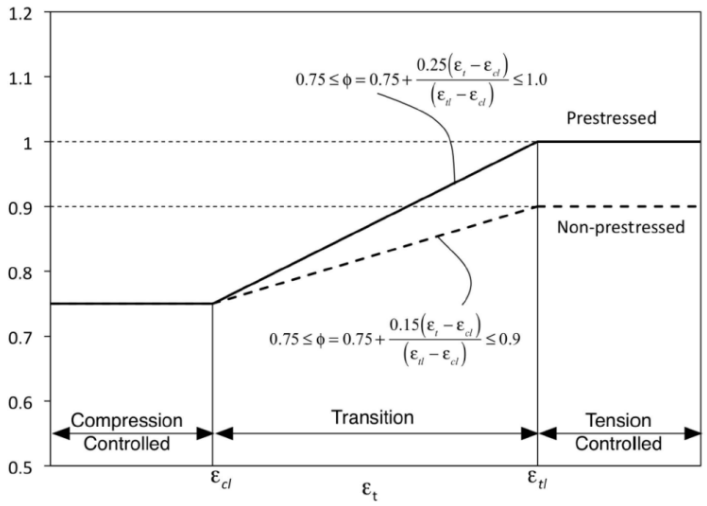

Figure 8 – (AASHTO LRFD Figure C5.5.4.2.1-1)

Where:

ε_t = net tensile strain in the extreme tension steel at nominal resistance

ε_{cl} = compression-controlled strain limit in the extreme tension steel (taken as 0.002 according to AASHTO LRFD 5.7.2.1)

ε_{tl} = tension-controlled strain limit in the extreme tension steel (taken as 0.005 according to AASHTO LRFD 5.7.2.1)

Service I Limit State

The Service I limit state relates to "concrete compressive stress in prestressed concrete components" (AASHTO LRFD Article 3.4.1). To satisfy this limit state, maximum concrete compressive stresses at a given section must not exceed $0.60f'_{ci}$ for construction stage I and $0.60f'_c$ for construction stages II and III, when the loads given by Eq. 6 are imposed on the structure. AASHTO LRFD states that the resistance factor $\phi = 1.0$ for all non-strength limit states (source).

$$1.00(DC + DW) + 1.00\,(LL + IM) \qquad \text{Eq. 6}$$

Where:

f'_c = specified compressive strength of concrete

f'_{ci} = compressive strength at the time of initial prestressing

Service III Limit State

The Service III limit state relates to "tension in prestressed concrete superstructures with the objective of crack control" (AASHTO LRFD Article 3.4.1) and is only checked for construction stage III loadings. To satisfy this limit state, maximum concrete tensile stresses at a given section must not exceed $0.0948\sqrt{f'_c}$ when the loads given by Eq. 7 are imposed on the structure.

$$1.00(DC + DW) + 0.80(LL + IM) \qquad \text{Eq. 7}$$

2.3 Design Checks and Construction Stages

Each girder was checked against each limit state at nineteen evenly spaced locations along the beam span as well as at the end of the transfer length of the prestressing strands. These checks were performed for three different construction stages devised to consider the variations in loading expected

during various stages of construction and use of the structure. The following briefly describes each of the three construction phases considered in this analysis.

Construction Stage I

Construction stage I includes the time from the release of prestressing strands (and thus transfer of prestressing strand force to the beam) and prior to casting of the bridge deck onsite. During this time the beam may be in the prestressing bed, in transportation to the construction site, or erected. During this construction stage the beam is non-composite. Only the dead load from beam self-weight was considered during this stage. The jacking stress of the prestressing strands was assumed to be $0.75f_{pu}$, and during construction stage I the stands were assumed to have experienced a loss in prestressing force due only to elastic shortening. These assumptions are consistent with KDOT Design Specifications.

For construction stage I the only limit state to evaluate is Service I because the Service I and III load combinations will result in the same loading with the absence of live load, and construction stage II has larger bending moment demands. To execute the service limit state checks, stresses were calculated in the top and bottom of the beam under the LRFD Service I load combination.

Construction Stage II

Construction stage II includes the time between casting of the bridge deck and development of full composite action between the deck and beam. Non-composite section properties were thus used. The loads acting on the beam during this stage included self-weight and the weight of the wet concrete deck and fillets. No live load forces were accounted for during construction stage II. Both the flexural capacity of the beam and beam stresses were checked for this stage. For these calculations, it was assumed that the prestressing strands had experienced all prestress losses and that the materials behaved linear-elastically.

Construction Stage III

Construction stage III begins when the beam achieves full composite action with the deck and extends for the remainder of the service life of the structure. Composite section properties for the beam were considered for this stage. The width of the concrete deck for the composite beam section of an interior beam was assumed equal to the effective flange width, which “may be taken as one-half the distance to the adjacent stringer or girder on each side of the component” per Article 4.6.2.6.1 of the AASHTO LRFD Specifications (AASHTO 2014).

The flexural demand and stresses from construction stage II loads are "locked" into the beam when it becomes composite. In addition to those demands, during construction stage III the beam will also support loads from the bridge railing, future wearing surface, and vehicular live loads and impact. The concrete deck portion of the composite beam will only experience loading from the bridge railing, future wearing surface, and vehicular load and impact.

For this construction stage the flexural capacity was checked for ultimate moment considering non-linear material behavior. For evaluating compliance with service limit states, beam stresses were calculated at the bottom and top of the precast section as well as at the top of the deck. No additional prestress losses were considered beyond those of construction stage II.

2.4 Loads

Dead Loads

The beam, deck, fillet, and railing were all considered structural components of the bridge and therefore were assumed to contribute to the total dead loads, *DC*, defined by the AASHTO LRFD specifications. The future wearing surface was considered a *DW* load. Effects from *DC* and *DW* loads were calculated based on material weights and the tributary width of the deck and converted to a uniform load distributed along the length of the beams. Moment and shear demand along the beam due to dead load was then calculated using Eqs. 8 and 9 respectively for a uniformly distributed load on a simple beam.

$$M_x = \frac{wx}{2}(l - x) \quad \text{Eq. 8}$$

$$V_x = w\left(\frac{l}{2} - x\right) \quad \text{Eq. 9}$$

Where:

M_x = moment at location x along beam

V_x = shear at location x along beam

w = distributed load

x = distance along beam

l = length of beam

The following provides greater detail regarding calculation of *DC* for each of the structural components listed above. In all cases, a concrete density of 0.145 kcf was assumed.

- Deck: The dead load from the bridge deck was calculated assuming a total deck thickness of 8.5 in. (the thickness of the deck assumed for calculation of flexural strength was assumed to be 8 in.

to account for a potential 0.5 in. reduction in thickness over time due to vehicular use, or sacrificial wear (KDOT 2016).

- Fillet: The fillet is the concrete area between the top of the beam and the bottom of the deck. The thickness of the fillet may vary along the length of the beam depending on beam camber, dead load deflection, and bridge final grade elevations. For prestressed beam bridges, KDOT specifies a minimum fillet depth of ½" and maximum of 4" (KDOT 2016). For the charts, the fillet thickness was assumed to be a constant 1.5 in. along the entire length of the prestressed beam.
- Bridge Rail: The bridge rail type used in practice varies based on the location of the bridge and how the deck drainage is handled. Standard weights for various rail systems can be found in the KDOT Bridge Design Manual (KDOT 2016). The option of either the 32" Kansas corral rail with or without curb or the 32" F-shape barrier with or without a 1½" overlay was included within the scope of this project.
- Future Wearing Surface (FWS): The FWS loads are meant to account for any overlays that may be added to the deck surface in the future. The KDOT Bridge Design Manual gives two options for the FWS load based on the amount of concrete cover for the top reinforcing steel in the deck (KDOT 2016, p. 3-3); 25 psf for 2.50 in. concrete cover and 15 psf for 3.00 in. concrete cover. Both options are included within the scope of this project.

Live Loads

The AASHTO HL-93 model for highway loads, developed in 1993, was used to evaluate live load effects in construction stage III. The AASHTO HL-93 model consists of three different live loads:

- Design truck (HS20): The design truck, shown in Figure 9, represents a typical semitrailer truck with an 8 kip front axle load, a 32 kip drive axle load located 14 ft behind the front axle, and a 32 kip rear axle load located at a variable distance ranging between 14 to 30 ft behind the drive axle. These loads are spaced to create a potentially critical load effect. This design truck is the same configuration that has been used by AASHTO (2002) Standard Specifications since 1944, commonly referred to as HS20 where H denotes highway, S denotes semitrailer, and 20 is the weight of the tractor in tons (Barker and Puckett 2007).

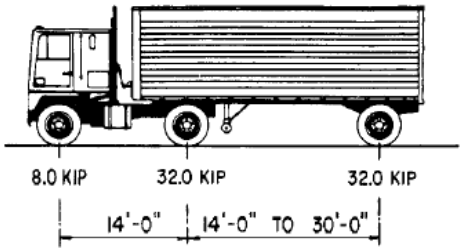

Figure 9 – AASHTO design truck loading (AASHTO LRFD 2014)

- Design tandem: The design tandem includes two 25 kip axle loads spaced at 4 ft.
- Design lane: The design lane is a uniformly distributed load of 0.064 kips/ft^2 along the length of the bridge occupying a region of 10 ft. transversely. Multiplying the distributed load by the transverse width results in 0.64 kips/ft, which was used for the lane load along the length of the beam.

For the AASHTO HL-93 model, both the design truck and design tandem live loads are superimposed with the design lane load and the combination that creates the most extreme load effects is used for design. According to AASHTO 2014 (reproduced as Table 4), an impact factor of 33% must be applied to truck loads for both strength and service limit state checks. This factor has been determined through numerous experimental and analytical studies of the dynamic load effect that occurs when the roughness of the roadway and the suspension system of the truck cause oscillation of the axle load above and below the static load.

Table 4 – Live load impact factors (AASHTO LRFD 2014 Table 3.6.2.1-1)

Component	IM
Deck Joints—All Limit States	75%
All Other Components:	
• Fatigue and Fracture Limit State	15%
• All Other Limit States	33%

The truck live load can occur along the bridge at any location and in either direction. Influence lines were used to find the maximum load effects at different points along the length of the bridge due to

movement of the truck load. Live load distribution factors were used to distribute these moments to each beam. Table 5 below shows the equations used to calculate the live load distribution factors.

Concrete Deck or Filled Grid, Partially Filled Grid, or Unfilled Grid Deck Composite with Reinforced Concrete Slab on Steel or Concrete Beams; Concrete T-Beams, T- and Double T-Sections	a, e, k and also i, j if sufficiently connected to act as a unit	One Design Lane Loaded: $0.06+\left(\frac{S}{14}\right)^{0.4}\left(\frac{S}{L}\right)^{0.3}\left(\frac{K_g}{12.0Lt_s^3}\right)^{0.1}$ Two or More Design Lanes Loaded: $0.075+\left(\frac{S}{9.5}\right)^{0.6}\left(\frac{S}{L}\right)^{0.2}\left(\frac{K_g}{12.0Lt_s^3}\right)^{0.1}$	$3.5 \le S \le 16.0$ $4.5 \le t_s \le 12.0$ $20 \le L \le 240$ $N_b \ge 4$ $10{,}000 \le K_g \le 7{,}000{,}000$
		use lesser of the values obtained from the equation above with $N_b = 3$ or the lever rule	$N_b = 3$

Table 5 - Live load distribution factor for moment in interior beams (AASHTO 2014)

Where, in Table 5:

S = spacing of beams or webs (ft)

L = span of beam (ft)

t_s = depth of concrete slab (in)

K_g = longitudinal stiffness parameter (in.^{4}), taken as $n(I + Ae_g^2)$ per AASHTO 4.6.2.2.1-1

$n = E_B/E_D$ per AASHTO 4.6.2.2.1-2

E_B = modulus of elasticity of concrete in the precast beam (ksi)

E_D = modulus of elasticity of concrete in the deck (ksi)

I = moment of inertia of non-composite beam (in^4)

e_g = distance between the centers of gravity of the beam and deck (in)

A = area of non-composite beam (in^2)

3. Discussion of Assumptions and Approach to Limit State Evaluation

3.1 Strength Limit State Calculations

The AASHTO LRFD Strength I load combination was used for the strength limit state check of the prestressed beams for this project. Mild reinforcing steel in the prestressed beam was not accounted for in these calculations. The beam section was assumed to be homogeneous. The flexural strength of the prestressed beams was checked for both construction stage II and III loadings. Only linear-elastic behavior of the beams was considered for the construction stage II strength check; non-linear material behavior was considered when checking the nominal moment capacity of the prestressed beam under Construction Stage III loading.

Beam theory was used to calculate the nominal flexural capacity of the prestressed beam. This method assumes strain compatibility, i.e. that plane sections prior to bending will remain plane during bending and that there is a perfect bond between the concrete and reinforcement. These assumptions work well for non-standard geometric sections like the NU girder and also when considering non-linear material behavior as long as shear deformations are limited (which is the case for standard bridge girders). For this strength check, the entire length of the beam was checked for the maximum moment. The use of strain compatibility for flexural design is also in compliance with the KDOT Bridge Design manual and AASHTO LRFD Specifications. Section 5.1.2.2 of the KDOT Bridge Design manual states that "for conventional strength design methods…strain compatibility may be used." Section 5.6.1 of the AASHTO LRFD Specifications also states under design considerations for concrete structures that "…equilibrium and strain compatibility shall be maintained in the analysis."

Strains in Concrete

Strain compatibility assumes that plane sections prior to bending will remain plane during bending and therefore the section experiences a linear strain distribution (Figure 10).

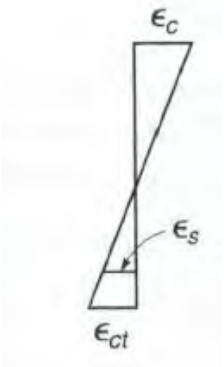

Figure 10 – Linear strain distribution in reinforced concrete section (Nilson, Darwin, Dolan 2010)

It has been observed that the nominal flexural strength of a beam can be reasonably approximated assuming the maximum compressive strain in the concrete section (ε_c in Figure 10) is 0.003 and enforcing equilibrium at the section. A straightforward method for enforcing equilibrium at a section when materials behave non-linearly is to divide the beam cross-section into layers representing both the concrete and reinforcement. The strain in each layer can be calculated representing either steel or concrete materials based on the assumed linear distribution of strain shown in Figure 12 using Eq. 10.

$$\varepsilon = \varepsilon_c \left(\frac{d-c}{c}\right) \quad \text{Eq. 10}$$

Where:

ε_c = maximum compressive strain in extreme compression fiber, assumed to be 0.003

d = depth of concrete section

c = depth of neutral axis

The stress in each layer can then be estimated based on the calculated strain using known stress-strain relationships for concrete and reinforcement. A commonly assumed model for relating concrete strain and stress is given in Eq. 11. Forces in each layer of the beam section can then be calculated from the estimated stress and known sectional area. Once the forces have been calculated in each layer and equilibrium satisfied, the moments from these forces can be summed up to find the nominal moment capacity of the beam.

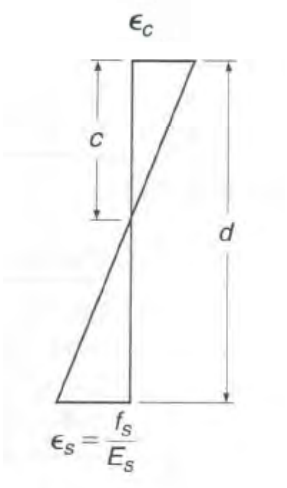

Figure 11 - Linear strain distribution in reinforced concrete section (Nilson, Darwin, Dolan 2010)

$$f_c = f'_c \left[\frac{2\varepsilon_{ci}}{\varepsilon_0} - \left(\frac{\varepsilon_{ci}}{\varepsilon_0}\right)^2\right] \text{ for } \varepsilon_{ci} \leq 0 \quad \text{Eq. 11}$$

Where:

ε_{ci} = strain in concrete layer

ε_0 = strain corresponding to f'_c

For the beams considered in this analysis, prestressing forces were always sufficiently large to preclude development of tensile strains in the concrete.

Strains in Prestressing Strands

The strain, ε_s, in the prestressing strands can be taken as the sum of three components (Figure 12 and Eq. 12).

$$\varepsilon_s = \varepsilon_1 + \varepsilon_2 + \varepsilon_3 \quad \text{Eq. 12}$$

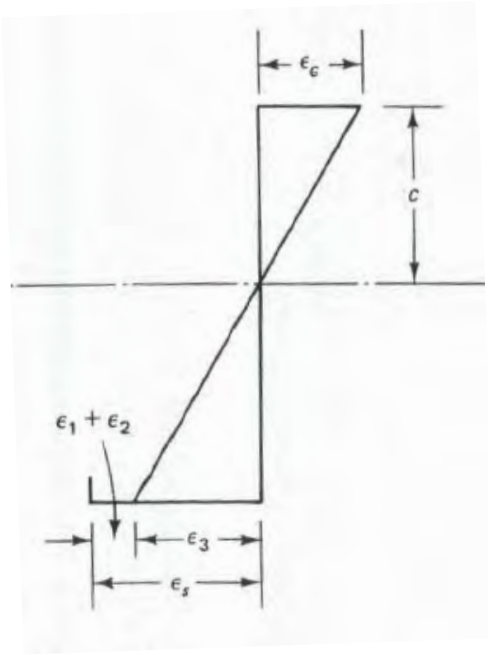

Figure 12 – Three components of strain in prestressing strands (Nawy 2006)

The first component of the strain, ε_1, represents the effective prestress force and can be calculated with Eq. 13.

$$\varepsilon_1 = \frac{f_{se}}{E_{ps}} \quad \text{Eq. 13}$$

Where:

f_{se} = effective prestressing force in strand

E_{ps} = modulus of elasticity of prestress strands

The second component of the strain, ε_2, can be calculated with Eq. 14. This strain component is meant to capture the effects of decompression, where the compressive stress in the concrete surrounding the prestressing strand is reduced by tensile stresses caused by loading of the prestressed section.

$$\varepsilon_2 = \frac{P_{se}}{E_c A_c} + \frac{P_{se} e^2}{E_c I_c} \quad \text{Eq. 14}$$

Where:

P_{se} = effective prestressing force = $f_{se} A_s$

A_s = total cross-sectional area of prestressing strands

A_c = area of concrete section

E_c = modulus of elasticity of concrete

e = eccentricity = distance from centroid of concrete section to centroid of strands

I_c = moment of inertia of concrete section

The third component of the strain in the prestressing strands, ε_3, accounts for tensile strains in the reinforcement that develop when the section is loaded beyond the decompression load. Since strain compatibility assumes a perfect bond between the concrete and the reinforcement, the strain in the concrete and reinforcement are assumed to be the same at the depth of the reinforcement. Assuming a linear strain distribution in the concrete section (Figure 11), ε_3 can be calculated with Eq. 15.

$$\varepsilon_3 = \varepsilon_c \left(\frac{d - c}{c} \right) \quad \text{Eq. 15}$$

Once the strain in the prestressing strands is calculated, the stress in the strands can be estimated. The PCI Design Handbook recommends the use of Eq. 16 for approximating the relationship between stress and strain for a typical 270 ksi 7-wire low-relaxation prestressing strand.

$$\text{For } \varepsilon_{ps} \leq 0.0086\text{: } f_{ps} = E_{ps}\varepsilon_{ps} \text{ (ksi)}$$
$$\text{For } \varepsilon_{ps} > 0.0086\text{: } f_{ps} = 270 - \frac{0.04}{\varepsilon_{ps} - 0.007} \text{ (ksi)} \quad \text{Eq. 16}$$

Additional strength check

Allowing for the debonding and harping of strands in prestressed beams requires a check of nominal flexural capacity along the entire length of the beam due to the change in center of gravity of the strands along the beam length. The AASHTO LRFD Specifications provide equations in Section 5.7.3, Eqs. 17 - 22 in this report, which can be used to calculate the nominal flexure resistance of a prestressed concrete section. As stated in Article 5.7.3.1.3b, a substitution of $A_{psb}f_{pu}+A_{psu}f_{pe}$ for $A_{ps}f_{pu}$ may be used in equations Eqs. 19 and 20 to account for the presence of both bonded and unbonded tendons in the beam, with f_{pe} being the effective stress in the strands after all losses. This article also states that the stress in the unbonded tendons may be conservatively taken as f_{pe} when calculating the nominal flexural resistance of the member. These values may then be used in Eqs. 17 and 18. Eq. 21 from AASHTO calculates the nominal flexural resistance, M_n, for flanged sections. According to AASHTO LRFD 5.7.3.2.3, for rectangular sections the nominal flexural resistance may be calculated using Eq. 21 where b_w is taken as b. Also for Eq. 21 and according to AASHTO Article 5.7.3.1.3b (AASHTO 2014), "the average stress in the prestressing steel shall be taken as the weighted average of the stress in the bonded and unbonded prestressing steel, and the total area of bonded and unbonded prestressing shall be used". For the specified compressive concrete strength, f'_c, in Eqs. 19-21, the lower compressive strength between the beam and deck was used based on AASHTO Article 5.7.3.2.6 and C5.7.3.2.6. Mild steel reinforcement was neglected for these calculations.

$$f_{ps} = f_{pu}\left(1 - k\frac{c}{d_p}\right) \quad \text{Eq. 17}$$

$$k = 2\left(1.04 - \frac{f_{py}}{f_{pu}}\right) \quad \text{Eq. 18}$$

For T-section behavior (neutral axis in web):

$$c = \frac{A_{ps}f_{pu} - \alpha_1 f'_c(b - b_w)h_f}{\alpha_1 f'_c \beta_1 b_w + kA_{ps}\frac{f_{pu}}{d_p}} \quad \text{Eq. 19}$$

For rectangular section behavior (neutral axis in flange):

$$c = \frac{A_{ps} f_{pu}}{\alpha_1 f'_c \beta_1 b + k A_{ps} \frac{f_{pu}}{d_p}}$$ Eq. 20

$$M_n = A_{ps} f_{ps} \left(d_p - \frac{a}{2}\right) + \alpha_1 f'_c (b - b_w) h_f \left(\frac{a}{2} - \frac{h_f}{2}\right)$$ Eq. 21

$$M_r = \varphi M_n$$ Eq. 22

Where:

A_{ps} = area of prestressing steel

A_{psb} = area of bonded prestressing steel

A_{psu} = area of unbonded prestressing steel

f_{ps} = average stress in prestressing steel at nominal bending resistance

d_p = distance from extreme compression fiber to the centroid of prestressing tendons

b = effective width of the flange

b_w = web width

β_1 = stress block factor, taken as 0.85 for specified concrete compressive strengths not exceeding 4.0 ksi (Section 5.7.2.2 AASHTO LRFD Specifications)

h_f = compression flange depth

α_1 = stress block factor, taken as 0.85 for specified concrete compressive strengths not exceeding 10.0 ksi (Section 5.7.2.2 AASHTO LRFD Specifications)

a = depth of equivalent stress block; $c \cdot \beta_1$

c = distance from extreme compression fiber to the neutral axis

M_n = nominal resistance

M_r = factored resistance

Both the transfer and development lengths of the prestressing strands were taken into account when checking the flexural resistance along the beam. Based on Article 5.11.4.1 of the AASHTO LRFD Specifications, "the stress in the prestressing steel may be assumed to vary linearly from 0 at the point where bonding commences to the effective stress after losses, f_{pe}, at the end of the transfer length" (AASHTO 2014). Per AASHTO 2014, the transfer length may be calculated as 60 times the diameter of the strands, d_b. The initiation point of bonding along the beam was altered for debonded strands.

Development length was calculated using Eq. 23 from AASHTO Article 5.11.4.3. Equations from AASHTO LRFD Figure C5.11.4.2-1, or Figure 13 in this report were used to calculate the stresses in the strands with the exception of assuming f_{pe} for unbonded strands beyond the transfer length.

$$l_d \geq \kappa(f_{ps} - \frac{2}{3} f_{pe}) d_b \qquad \text{Eq. 23}$$

Where:

l_d = development length

κ = 1.6 (bonded strands), 2.0 (if unbonded strands included in design)

d_b = nominal strand diameter

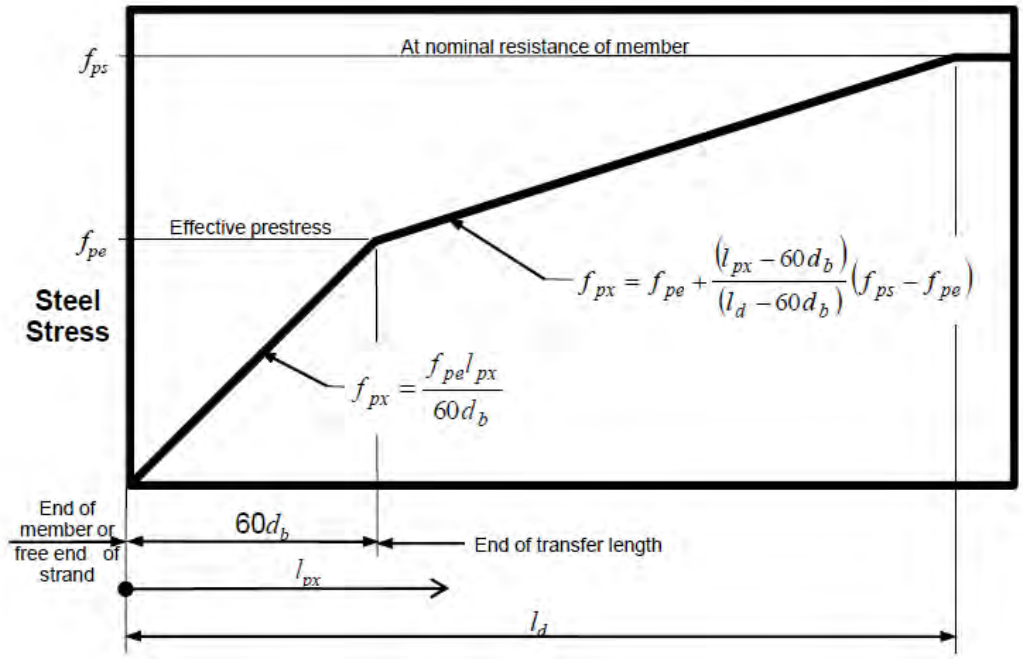

Figure 13 – AASHTO LRFD Figure C5.11.4.2-1

3.2 Service Limit State Calculations

Beam Longitudinal Stresses

Figure 14 shows how prestressing force and the location of the prestressing strands can change the stress distribution in a prestressed concrete beam.

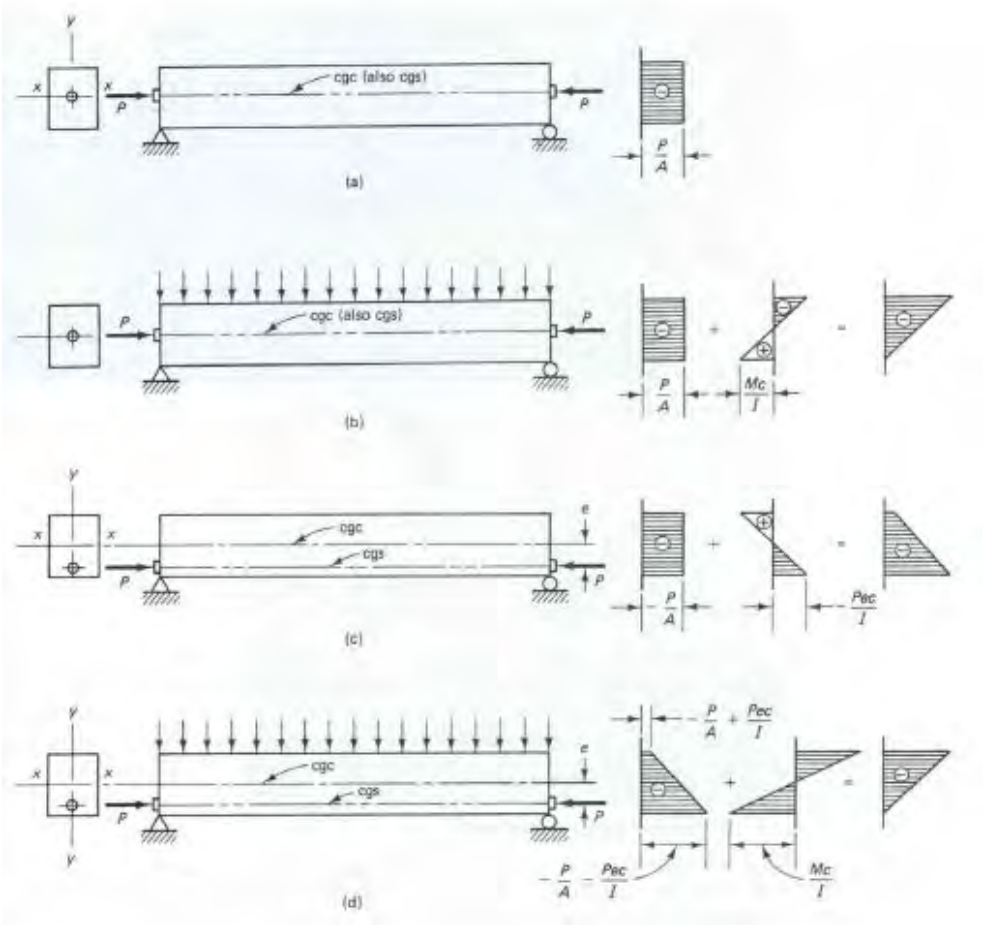

Figure 14 – Stress distribution in prestressed concrete beam (Nawy 2006)

When a concrete beam is subjected to a concentric prestressing force, as shown is Figure 14(a), the compressive stress on the beam cross section has an intensity given by Eq. 24.

$$f = -P/A_c \qquad \text{Eq. 24}$$

Where:

f = compressive stress on beam crosssection

P = prestressing force

A_c = cross-section area of beam

The self-weight and external transverse loads applied to a beam cause a maximum moment, M, at midspan. The distribution of this stress at a given section of the beam is shown in Figure 14(b). The

beam experiences compressive stress in the top and tensile stress in the bottom. These stresses can be calculated with Eq. 25.

$$f_t = -Mc/I_g$$
$$f_b = Mc/I_g \quad \text{Eq. 25}$$

Where:

f_t = stress at top of section

f_b = stress at bottom of section

M = maximum moment at midspan

c = distance from extreme beam fiber under consideration to centroid of beam section

I_g = gross moment of inertia of the section

It can be seen in Figure 14(b) that the compressive stresses in the top of the beam due to concentric prestressing force and external loads are additive. It is more efficient to place prestressing strands below the neutral axis at midspan so that tensile stresses are induced in the top of the beam, where external loads cause increased compression. Likewise, this placement of strands also results in increased compression along the bottom of the section, where external loads cause increased tension. There is thus an eccentricity, e, between the center of gravity of the beam and the center of gravity of the prestressing strands, which creates a moment, Pe. The stresses caused at midspan by the eccentric placement of strands can be calculated with Eq. 26.

$$f_t = Pec/I_g$$
$$f_b = -Pec/I_g \quad \text{Eq. 26}$$

For the case of combined prestressing and external forces, the stresses at midspan in the top and bottom beam fibers of a prestressed concrete section may be calculated using Eq. 27.

$$f_t = \frac{-P}{A} + \frac{Pey}{I} - \frac{My}{I}$$
$$f_b = \frac{-P}{A} - \frac{Pey}{I} + \frac{My}{I} \quad \text{Eq. 27}$$

Debonding and Harping of Strands

Strands may be debonded at the ends of prestressed concrete beams to control compressive stresses due to the prestressing force. Strands may also be harped to reduce compressive stresses in the bottom of a beam and tensile stresses in the top near the end of a beam. The KDOT Bridge Design Manual recommends the engineer consider use of parallel prestressed strands whenever possible, especially for shorter beams. When service and strength limits cannot be satisfied with parallel strands, the KDOT Bridge Design Manual recommends the engineer consider debonding strands near the ends of beams and, as a last resort, consider harping strands. Harped strands are the least preferred option due to the high hold-down force required during manufacture (local manufacturers have stated there are safety concerns associated with use of harped strands, (personal communication). Another option available to engineers is to include strands along the tops of beams, either fully or partially prestressed, to reduce top tensile stresses at the ends of the beams. The addition of up to eight strands in the tops of beams has been recommended by local prestressing manufacturers as an option that is more economical than harped strands.

Prestressing strands are debonded by encasing the strand in a plastic sheath along a certain length. The KDOT Bridge Design manual states that strands are typically debonded in 5 ft. increments. The following requirements are given by KDOT for debonded strands:

- Do not debond strands which will be extended
- Not more than 40% of the strands at one horizontal row will be debonded
- Not more than 25% of the total strands can be debonded
- The exterior strands of each horizontal row shall be fully bonded
- Symmetric debonding about member centerline is required
- Not more than 40% of the debonded strands, or four strands, whichever is greater, shall have the debonding terminated at a section
- Shear investigation shall be made in regard to the reduced horizontal force

When incorporating strand debonding into stress calculations, both the prestressing force and the location of the centroid of the force, and therefore the eccentricity, will change. The incorporation of transfer length into the beam stress equations will not occur until the bond between the concrete and the strand is initiated.

When harping strands, the harped strand hold-down points are normally located at the 0.4 and 0.6 pts. along the beam. KDOT limits the hold-down force per strand to 4 or 5 kips and total force for the hold-down device to 38 or 45 kips for 0.5 in. and 0.6 in. diameter strands respectively. Section 5, Appendix B of the KDOT Bridge Design Manual provides Eqs. 28 - 31 for calculating the hold-down forces required for harped strands:

$$\varphi = \left(atan\left(\frac{e}{L_b \cdot Harp \cdot 12}\right)\right) \cdot \frac{360}{2\pi} \quad \text{Eq. 28}$$

$$\beta = 90 - \varphi \quad \text{Eq. 29}$$

$$\text{hold down force per strand (kip)} = \frac{2}{Harp_n} \cdot P_u \cdot \cos\left(\frac{2\pi}{360} \cdot \beta\right) \quad \text{Eq. 30}$$

total hold down force for device (kip) = hold down force per strand $\cdot N_s$ Eq. 31

Where:

e = strand eccentricity

L_b = beam length

$Harp$ = harp location (tenth point)

$Harp_n$ = number of harp locations (typically two)

φ = angle for harp from horizontal

β = angle for harp from vertical

N_s = number of strands

Stress Limits

Table 6 shows the concrete stress limits permitted for service limit state according to KDOT Design Specifications for prestressed beams. Without the consideration of debonded or harped prestressing strands in the beam design, the NU girder span lengths were limited by excessive tensile stresses towards the ends of the beams for both initial and final construction stages. Beam stresses during shipping and handling stages were not considered in this project.

Table 6 – KDOT LRFD design concrete stress limits (ksi) at service limit states

Stage	Stresses, (ksi)	*Article (s)*
Initial Compression	$0.60 f'_{ci}$	5.9.4.1.1
* Initial Tension	$0.24\sqrt{f'_{ci}}$	5.9.4.1.2
Final Compression	$0.60 f'_{c}$	5.9.4.2.1
Final Tension	$0.0948\sqrt{f'_{c}}$	5.9.4.2.2
Final DL Compression	$0.45 f'_{c}$	5.9.4.2.1
Shipping & Handling Compression	$0.60 f'_{c}$	5.9.4.2.1
* Shipping & Handling Tension	$0.24\sqrt{f'_{c}}$	5.9.4.1.2

* Where A_s is proportioned as stated in *Article C.5.9.4.1.2*

3.3 Other Considerations

Prestress Losses

Both instantaneous and long-term time-dependent prestress losses must be accounted for in the design of prestressed beams. Instantaneous losses are assumed to occur before the concrete deck is placed, whereas long-term time-dependent losses occur after deck placement. According to the KDOT Bridge Design manual, total prestress losses may be calculated with Eq. 32.

$$\Delta f_{pT} = \Delta f_{pES} + \Delta f_{pLT} \qquad \text{Eq. 32}$$

Where:

Δf_{pT} = total losses

Δf_{pES} = instantaneous losses due to elastic shortening of the concrete (before deck placement)

Δf_{pLT} = long-term time-dependent losses due to creep, shrinkage and relaxation of the steel (after deck placement)

Only elastic shortening is considered when calculating instantaneous prestress losses. Eq. 33 is given in AASHTO LRFD C5.9.5.2.3a-1 for calculating losses due to elastic shortening.

$$\Delta f_{pES} = \frac{A_{ps} f_{pbt}\left(I_g + {e_m}^2 A_g\right) - e_m M_g A_g}{A_{ps}\left(I_g + {e_m}^2 A_g\right) + \frac{A_g I_g E_{ci}}{E_p}} \qquad \text{Eq. 33}$$

Where:

A_g = gross area of section (in^2)

E_{ci} = modulus of elasticity of concrete at transfer of prestressing force (ksi)

E_p = modulus of elasticity of prestressing strands (ksi)

e_m = average prestressing steel eccentricity at midspan (in)

f_{pbt} = stress in prestressing steel immediately prior to transfer (ksi)

I_g = moment of inertia of the gross concrete section (in^4)

M_g = midspan moment due to member self-weight (kip-in)

The effects of creep and shrinkage of the concrete as well as relaxation of the prestressing strands are all considered when calculating the long-term time-dependent prestress losses. KDOT uses AASHTO LRFD Specifications equation 5.9.5.3-1, reproduces as Eq. 34, to estimate time-dependent losses.

$$\Delta f_{pLT} = 10\frac{f_{pi}A_{ps}}{A_g}\gamma_h\gamma_{st} + 12\gamma_h\gamma_{st} + \Delta f_{pR} \qquad \text{Eq. 34}$$

Where:

$\gamma_h = 1.7 - 0.01H$

$\gamma_{st} = \frac{5}{(1+f'_{ci})}$

f_{pi} = prestress steel stress immediately prior to transfer (ksi)

H = average annual ambient relative humidity (%), use 65% for Kansas

γ_{st} = correction factor for specified concrete strength at time of prestress transfer

γ_h = correction factor for relative humidity of the ambient air

Δf_{pR} = loss due to relaxation of steel after transfer (ksi), an estimate of 2.4 ksi is taken for low relaxation strands

Table 5.9.3-1 of AASHTO LRFD limits the stress in the prestressing strands immediately prior to transfer to $0.75f_{pu}$ and at service limit states after all losses, f_{pe}, to $0.80\ f_{py}$, for low relaxation strand.

Shear

Due to the potential for adding shear reinforcement in a beam wherever necessary, shear design would not control the span capacities for the design charts. However, AASHTO LRFD specifies an upper limit of nominal shear resistance, V_n, in Article 5.8.3.3. Eq. 35 is given in AASHTO LRFD to calculate this upper limit. The shear demand along the beam was calculated and appropriate LRFD Strength I load and resistance factors were applied.

$$V_n = 0.25 f_c' \, b_v \, d_v + V_p \qquad \text{Eq. 35}$$

Where:

$$d_v = \frac{M_n}{A_{ps} f_{ps}}$$

b_v = effective web width taken as the minimum web width within the depth d_v

d_v = effective shear depth; it need not be taken to be less than the greater of $0.9d_e$ or $0.72h$ (AASHTO LRFD C5.8.2.9-1)

d_e = effective depth from extreme compression fiber to the centroid of the tensile force in the tensile reinforcement

$$d_e = \frac{A_{ps} f_{ps} d_p}{A_{ps} f_{ps}}$$

h = overall thickness or depth of a member

V_p = component in the direction of the applied shear of the effective prestressing force; $V_p = 0$ when AASHTO LRFD Article 5.8.3.4.3 is applied

4. Design Charts

4.1. Example Charts

Figures 14 and 15 are examples of the NU girder design charts that may be generated from this project. Tables 7 and 8 give details of these charts in a tabular format. An Excel spreadsheet was created considering all of the calculations described in this report giving KDOT the ability to generate charts like Figures 14 and 15 considering all NU girder sections, span lengths, beam spacings, number of prestressing strands, and final compressive strengths of concrete included in the scope of this project. Figure 14 shows an example chart of span capacities of NU girder sections with respect to beam spacing and beam final compressive strength of concrete of 8 ksi. This type of chart aids engineers in choosing a preliminary NU girder section for a desired span length and beam spacing. Figure 15 shows an example chart that is

specific to a single NU girder section, allowing the engineer to choose a preliminary number of prestressing strands for their design based on span length and beam spacing. Calculations were checked using AASHTOWare Bridge Design (BrD) software.

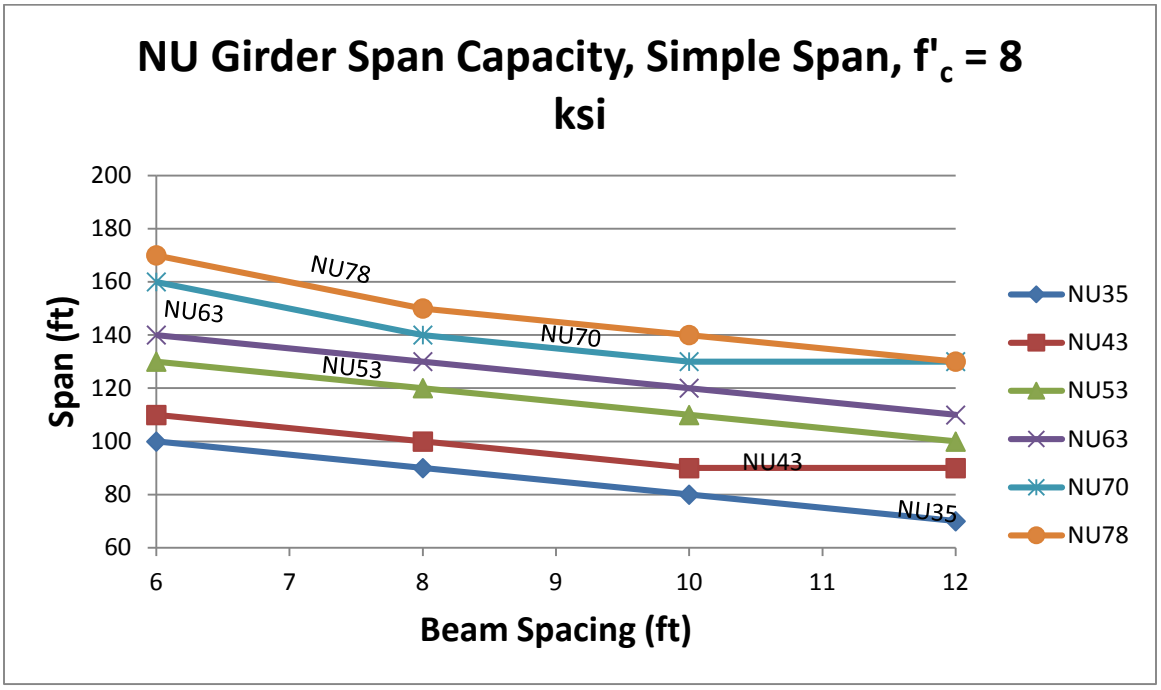

Figure 14 – Example of NU girder span capacity design chart

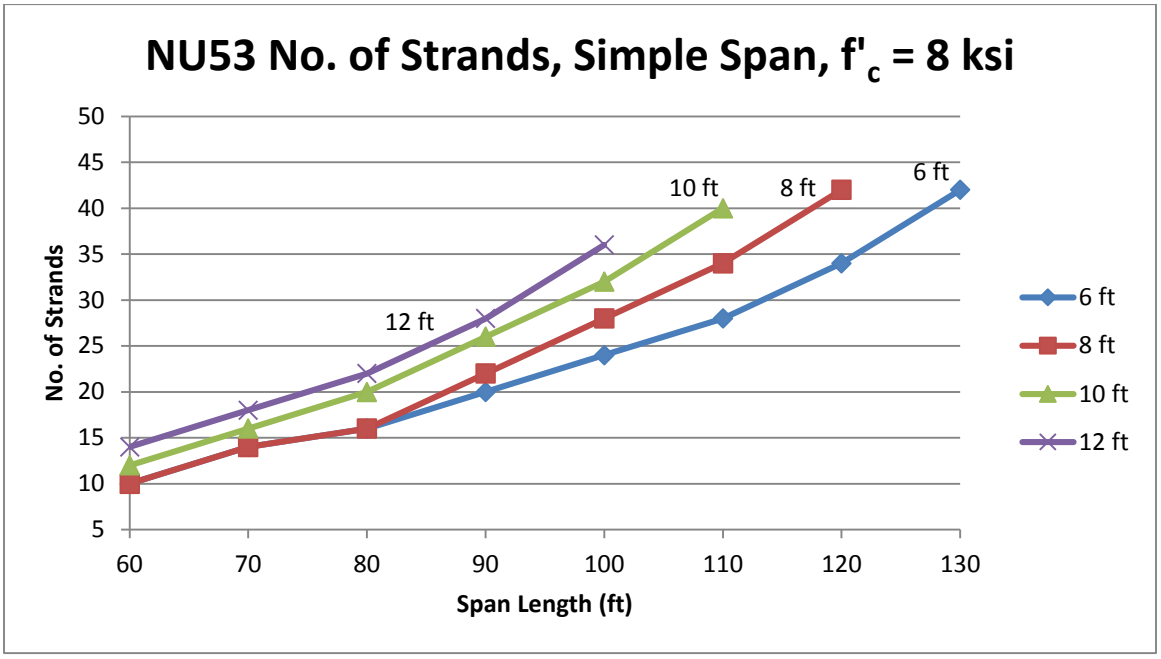

Figure 15 – Example of NU girder no. of strands design chart

Table 7 – NU girder span capacity and minimum number of strands

NU Girder Span Capacity, Simple Span, f'c = 8 ksi			
Beam Section	**Beam Spacing (ft)**	**Span (ft)**	**Min. no. of strands**
NU35	6	100	36
	8	90	34
	10	80	30
	12	70	26
NU43	6	110	36
	8	100	34
	10	90	32
	12	90	36
NU53	6	130	42
	8	120	42
	10	110	40
	12	100	36
NU63	6	140	40
	8	130	40
	10	120	40
	12	110	36
NU70	6	160	48
	8	140	42
	10	130	42
	12	130	48
NU78	6	170	50
	8	150	44
	10	140	44
	12	130	42

Table 8 – NU53 minimum number of strands for girder spacing and span length

NU53 No. of Strands, Simple Span, f'_c = 8 ksi		
Girder Spacing (ft)	**Span Length (ft)**	**Min. no. of strands**
6	130	42
6	120	34
6	110	28
6	100	24
6	90	20
6	80	16
6	70	14
6	60	10
8	120	42
8	110	34
8	100	28
8	90	22
8	80	16
8	70	14
8	60	10
10	110	40
10	100	32
10	90	26
10	80	20
10	70	16
10	60	12
12	100	36
12	90	28
12	80	22
12	70	18
12	60	14

5. Summary

In anticipation of the adoption of NU girder sections for in-house bridge design projects, KDOT desired charts to aid in the preliminary design of these beams. An Excel spreadsheet was developed to perform the necessary LRFD design checks on the NU girder sections. This Excel tool may be used to generate the NU girder design charts desired by KDOT.

5.1. Future Work

The scope of this project was limited to the range of parameters listed in Section 2.1. Modifications that increase the range of parameters that can be considered, including applicability to continuous bridge structures, and the option to use partially prestressed strands in the tops of the beams, would be beneficial additions for KDOT engineers. Incorporating these options into the Excel spreadsheet used for the calculations on this project would help create a more comprehensive preliminary design tool.

REFERENCES

AASHTO LRFD Bridge Design Specifications, Seventh Edition, 2014 U.S. Customary Units w/2015 Interims, 2014, Washington, D.C.

Barker, R. M., and Puckett, J. A. (2007). *Design of Highway Bridge, An LRFD Approach, Second Edition*, Hoboken, NJ.

Hanna, K. E., Morcous, G., and Tadros, M. K. (2010). *Design Aids of NU I-Girder Bridges*, Final Report to Nebraska Department of Roads, Project No. P322.

Darwin, D., Dolan, C. W., and Nilson, A. H. (2010). *Design of Concrete Structures, Fourteenth Edition*, New York, NY.

KDOT (Kansas Department of Transportation). (2016). *Design Manual Volume III – Bridge Section*, Topeka, KS.

Nawy, E. G. (2006). *Prestressed concrete: a fundamental approach*, Upper Saddle River, NJ, Chapter 1, pp. 7-10.

NDOR (Nebraska Department of Roads). (2014). *Bridge Office Policies and Procedures,* Lincoln, NE.

PCI (Precast/Prestressed Concrete Institute). (1999). *PCI Design Handbook, Fifth Edition*, Chicago, IL.